Chinese Chemical Letters 34 (2023) 108108

Contents lists available at ScienceDirect

Chinese Chemical Letters

journal homepage: www.elsevier.com/locate/cclet

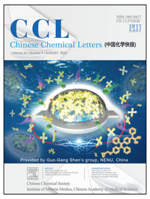

Photoisomerization, assembling and fluorescence photoswitching behaviors of a water-soluble stiff-stilbene with cucurbit[7]uril

Liangru Yang[a,*], Yixin Li[a], Haifan Zhang[a], Changming Tian[b], Qiaohong Cao[a], Yongmei Xiao[a], Libo Yuan[a,*], Guoxing Liu[a,b,*]

[a] *College of Chemistry and Chemical Engineering, Henan University of Technology, Zhengzhou 450001, China*
[b] *College of Science, Henan Agricultural University, Zhengzhou 450002, China*

ARTICLE INFO

Article history:
Received 24 September 2022
Revised 20 December 2022
Accepted 25 December 2022
Available online 26 December 2022

Keywords:
Supramolecular assemble
Photoreponse
Stiff-stilbene
Cucurbit[7]uril
Fluorescence photoswitch
Host-guest complexation

ABSTRACT

Photoresponsive supramolecular systems have merited extensive attention for their applications in materials science and life science. Here, we synthesized a water-soluble stiff-stilbene molecular photoswitch, exhibiting outstanding photoisomerization reaction between its (*E*)- and (*Z*)-configurations upon irradiation at distinct light. The photoswitch can assemble with cucurbit[7]uril (CB[7]) to form a superior fluorescent supramolecular complex (compared to the only guest) with excellent water solubility, which manifested dramatic photoluminescence enhancement caused by restriction of intramolecular rotation and remained good photochromic characteristics. Furthermore, introduction of CB[7] influence photoreaction quantum yield (Φ) of the stiff-stilbene, leading to reduction of $\Phi_{E\rightarrow Z}$ and increase of $\Phi_{Z\rightarrow E}$ of the stiff-stilbene. Importantly, the photoadjustable supramolecular assembly can act as a fluorescence switch, and the phototunable guest further selectively modulate G-quadruplex structure of Tel22 upon light irradiation or with addition of CB[7]. The study provides a new simple way for accurately regulating photochromic properties of molecular switches and developing smart materials with potential applications in controlled modulation of G-quadruplex, targeted biological imaging and so on.

Stimulus responses are ubiquitous in nature. For imitating biofunctionability, numerous stimuli-responsive systems have been fabricated and used for molecular machines [1–3], drug delivery [4], controlled ion channel [5] and intelligent photoluminescence [6–12]. In recent years, supramolecular self-assembly sprang up and became a simple and convenient method to construct the stimuli-responsive systems, because weak noncovalent effects among them are more easily and regularly controlled. Thereinto, supramolecular interactions are reversibly destroyed and rebuilded encountering external stimulus such as acid-base, temperature, pressure, light, magnetism [13–19]. Among them, preference for light over other ones is attributed to its inherent advantages such as ubiquity, controllability and noninvasion [20]. Recently, photosensitive systems are increasingly built for developing light-induced self-healing gel [21], photomodulated conductive device [22], photocontrolled bioimaging [23], high-security-level anti-counterfeiting [24], switching reactive oxygen [25,26] and photoadjusted mechanical motion [27]. Generally, photoactive molecules such as diarylethene, azobenzene, spiropyrane and stiff-stilbene, resemble a motor, where light is a fuel, which constitute indispensable basic element of photosensitive systems. In-depth understanding mechanism of photoactivity and advance of new molecular photoswitches appear to be particularly significant. Stiff-stilbene derivatives can undergo isomerization between (*E*)- and (*Z*)-configuration upon distinct light, where dramatical change of geometric configuration take place [28]. In view of this, Feringa and co-workers developed a series of functional stiff-stilbene receptors bearing bisurea, which could stereoselectively bind phosphate [29–31]. Later, we also reported a new bisurea-modified stiff-stilbene, manifesting controlled release phosphate and carbonate [32].

Cucurbit[*n*]urils (CB[*n*]), a common class of macrocyclic hosts with rigid cavities, can encapsulate positively charged guests or charge-transfer complexes through electrostatic and hydrophobic interaction to self-assemble into stable regular host–guest complexes [33]. CB[*n*] as a modulator has been employed to regulate photoisomerization reaction and photoluminescence behaviors of resultant diarylethene derivatives with a particular structure [34,35]. Nevertheless, it has been not exploited yet that sufficient utilization of structural peculiarities of CB[*n*] regulated

---

[*] Corresponding authors.
E-mail addresses: lryang2003@aliyun.com (L. Yang), lbyuan@haut.edu.cn (L. Yuan), gxliu@henau.edu.cn (G. Liu).

https://doi.org/10.1016/j.cclet.2022.108108
1001-8417/

photochromic and photoluminescent characteristics of the stiff-stilbene molecular photoswitches *via* supramolecular self-assembling way, to the best of our knowledge. Herein, a water-soluble stiff-stilbene salt as a guest was tactfully designed and expediently assembled with CB[7] to form 1:2 supramolecular complex. The intervention of CB[7] could obviously enhance photoluminescence performance and modulate photochromic properties of the guest *via* restriction of intramolecular rotation induced by self-assembly and simultaneously, the supramolecular complex exhibited controllable fluorescence switching behaviors. Furthermore, remarkable water-solubility and biocompatibility provided the possibility for further implementation of stimuli-responsive function in bioscience field.

Water-soluble stiff-stilbene phenyl derivatives (*E*)-WS-SSP and (*Z*)-WS-SSP were designed and synthesized through several simple steps, as displayed in Scheme S1 (Supporting information). (*E*)-SS-Br and (*Z*)-SS-Br were prepared according to the reported literature [27], and further reacted with 4-formylphenylboronic acid under catalysis of $Pd(PPh_3)_4$ though Suzuki coupling reaction to afford (*E*)-SSP-NH_2 and (*Z*)-SSP-NH_2 [36]. Subsequently, the two amines were further methylated and anion-exchanged to obtain water-soluble stiff-stilbene phenyl quaternary ammonium salts (*E*)-WS-SSP and (*Z*)-WS-SSP. Their chemical compositions were characterized by ^{1}H NMR, ^{13}C NMR and HR-MS (Figs. S1-S6 in Supporting information).

As is well-known, stiff-stilbenes can be isomerized between their (*E*)- and (*Z*)-configurations upon irradiation at distinct light. As displayed in Fig. S7a (Supporting information), the UV-vis absorption spectrum of (*E*)-WS-SSP revealed larger absorbance between 300 nm and 350 nm than that of its (*Z*)-isomer, while its (*Z*)-isomer manifested greater absorbance between 360 nm and 405 nm. Therefore, we employed 311 nm light to induce isomerization of WS-SSP from (*E*)- to (*Z*)-isomer, and selected 385 nm light to conduct the reverse process. As shown in Fig. 1a, the maximum absorption peaks of (*E*)-WS-SSP at 267 nm, 334 nm and 350 nm decreased, and the absorption band between 360 nm and 405 nm increased, upon irradiation at 311 nm ultraviolet (UV) light, manifesting the generation of a new substance, *i.e.*, (*Z*)-WS-SSP. Photostationary state (PSS) was reached after irradiation at 311 nm light for 30 s. As shown in Fig. S7a, UV-vis absorption spectra of its two configurations unreservedly validated the aforementioned inference. Subsequently, irradiation of the resultant sample at 385 nm light resulted in the restoration of original absorption spectrum to some extent (Fig. 1b). Afterwards, we performed three cyclic experiments through UV-vis absorption spectral variation upon irradiation at alternating 311 nm and 385 nm light, indicating acceptable photoisomerization reversibility (Fig. S8 in Supporting information). It is well known that photoreaction quantum yield (Φ) is an important parameter of photochemical reaction. $\Phi_{E\rightarrow Z}$ and $\Phi_{Z\rightarrow E}$ of WS-SSP were determined to be 12.38% ± 0.04% and 3.46% ± 0.05%, respectively, and their detailed tests were elaborated in Supporting information. Meanwhile, PSS_{311} and PSS_{385} ratios were determined by integration of the NMR signals as (*E*/*Z*) 55:45 and 72:28, respectively (Fig. S9 in Supporting information). The photoisomerization mechanism of the free guest WS-SSP was similar to that reported previously [36].

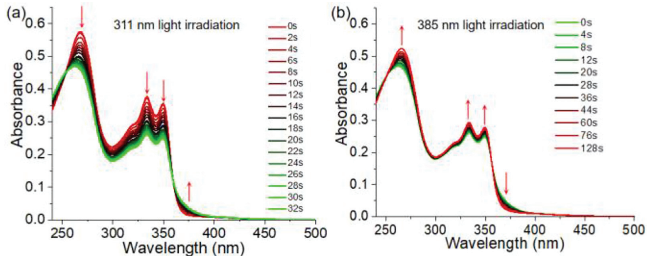

Fig. 1. (a) UV-vis absorption spectral variation of (*E*)-WS-SSP upon irradiation at 311 nm light; (b) UV-vis absorption spectral variation of a upon irradiation at 385 nm light; [(*E*)-WS-SSP] = 2×10^{-5} mol/L.

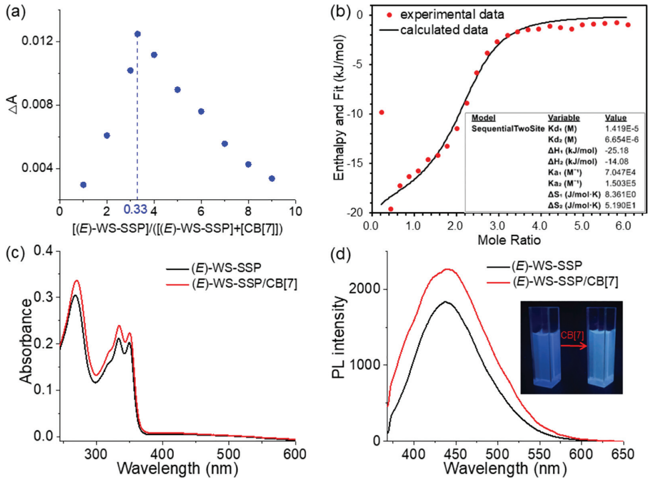

Fig. 2. (a) Job plot for (*E*)-WS-SSP upon complexation with CB[7] in aqueous solution at 25 °C; Absorption changes recorded at 350 nm for (*E*)-WS-SSP; The sum of the total concentrations of hosts and guests is constant (2.0×10^{-5} mol/L). (b) "Net" heat effects of complexation of (*E*)-WS-SSP/CB[7] for each injection, obtained by subtracting the dilution heat from the reaction heat, which was fitted by computer simulation with using the "1:2 sequential binding sites" model; The thermodynamic data in (*E*)-WS-SSP/CB[7] complexation were obtained as $K_{S1} = 7.0\times10^4$ L/mol, $K_{S2} = 1.5\times10^5$ L/mol, $\Delta H_1 = -25.18$ kJ/mol, $\Delta H_1 = -14.08$ kJ/mol, $T\Delta S_1 = 2.49$ kJ/mol, $T\Delta S_2 = 15.47$ kJ/mol, $\Delta G_1 = -27.67$ kJ/mol, and $\Delta G_2 = -29.55$ kJ/mol, respectively. (c) UV-vis absorption spectra of (*E*)-WS-SSP and (*E*)-WS-SSP/CB[7], [(*E*)-WS-SSP] = 1.0×10^{-5} mol/L. (d) Photoluminescence spectra of (*E*)-WS-SSP and (*E*)-WS-SSP/CB[7]; [CB[7]] = 2[(*E*)-WS-SSP] = 4.0×10^{-5} mol/L.

Possessing good water solubility and specific structural features, assembling behaviors of (*E*)-WS-SSP and CB[7] were subsequently studied in detail. A Job plot was performed to verify their optimum complexing stoichiometric ratio, where a maximum peak at a molar ratio of 0.33 was observed, manifesting a 2:1 host–guest complex stoichiometry (Fig. 2a). After confirming the binding stoichiometry, the complex stability constant (K_s) was calculated as 7.0×10^4 L/mol (K_{S1}) and 1.5×10^5 L/mol (K_{S2}) at 25 °C using isothermal titration calorimetry (ITC) testing (Fig. 2b and Fig. S17 in Supporting information). When CB[7] was added sequentially into the sample containing (*E*)-WS-SSP, all of its absorption peaks at 267 nm, 334 nm and 350 nm exhibited gradually increased (Fig. 2c and Fig. S10 in Supporting information), implying the occurrence of their assembling process. To verify the assembly model, the nuclear magnetic contrast and titration experiments were subsequently executed as shown in Fig. 3 and Fig. S11 (Supporting information). An apparent upfield shift for the resonance of the benzene ring protons (H_b and H_c) and a downfield shift for the protons in stiff-stilbene skeletons (H_{d-h}) were observed clearly, revealing that phenyl groups adjacent to quaternary ammonium salts were encapsulated by the cavity of CB[7] and stiff-stilbene and quaternary ammonium salts moieties were located out of CB[7]. Therefore, their assembling pattern was illuminated in Scheme 1 that a simple 2:1 supramolecular assembly (*E*)-WS-SSP/CB[7] formed.

Interestingly, upon sequential addition of CB[7], fluorescence intensity of water-soluble (*E*)-WS-SSP at 440 nm was dramatically enhanced, attributed to the restriction of intramolecular rotation induced by encapsulation of CB[7] (Fig. 2d and Fig. S12 in Supporting information). Visually, the fluorescence photograph of (*E*)-WS-SSP under 365 nm UV light became more bright obviously

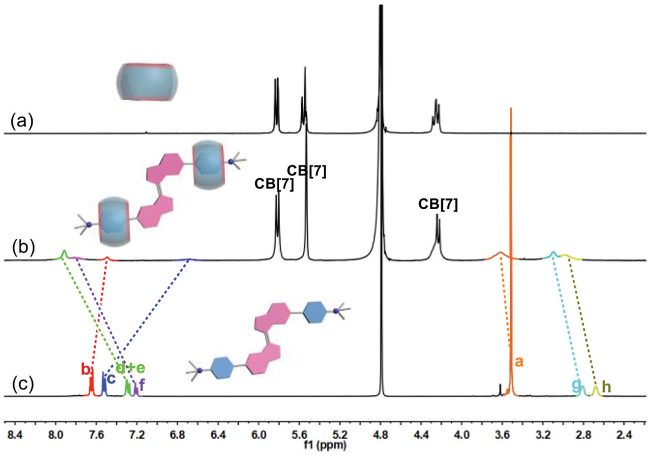

Fig. 3. The ^{1}H NMR (400 MHz, 298 K, D_2O) spectra of CB[7] (a), assembly (*E*)-WS-SSP/CB[7] (b) and (*E*)-WS-SSP (c). 2[(*E*)-WS-SSP] = [CB[7]] = 2.0×10^{-3} mol/L.

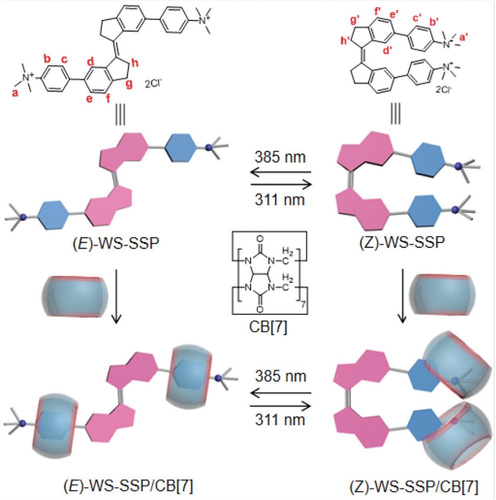

Scheme 1. Schematic illustration for assembling pattern of (*E*)-WS-SSP and CB[7], and photoisomerization of guest WS-SSP and assembly WS-SSP/CB[7].

with addition of 2 equiv. CB[7] (Fig. 2d, inset). Furthermore, maximum emission peak of the guest displayed bathochromic-shift from 436 nm to 440 nm originated from introduction of CB[7]. Meanwhile, these above phenomena also jointly manifested the successful construction of the (*E*)-WS-SSP/CB[7] assembly. Remarkable fluorescence enhancement enabled supramolecular assembly (*E*)-WS-SSP/CB[7] to be a satisfactory photoluminescent material.

Benefiting from good photochromic characteristics of WS-SSP, the assembly (*E*)-WS-SSP/CB[7] also possessed excellent photoisomerization properties. As shown in Fig. S13 (Supporting information), when it was irradiated by 311 nm light, the absorbance maximum at 267 nm, 334 nm and 350 nm gradually declined and meanwhile, the absorption band between 360 nm and 450 nm was apparently enhanced. Encapsulation of CB[7] on (*E*)-WS-SSP induced the absorbance of the guest at 267 nm, 334 nm and 350 nm to increase, as shown in Fig. 2c. If CB[7] disassembled with the guest, only the absorbance of (*E*)-WS-SSP would be decreased but the absorption band between 360 nm and 450 nm did not increase. Therefore, irradiation of the assembly at 311 nm light should lead to photoisomerization of (*E*)-WS-SSP/CB[7] to its (*Z*)-form and alteration of binding pattern of the assembly, as illuminated in Scheme 1. Subsequently, irradiation of the resultant sample at 385 nm light enabled the absorption to be recovered to some extent. Importantly, the above process could be repeated for three cycles without any major recession. Although the photoisomerization speed of the assembly from (*E*)-configuration to (*Z*)-configuration was inferior to that of the only guest due to the influence of CB[7], reversible photoisomerization of WS-SSP/CB[7] between (*E*)-form and (*Z*)-form could still occur. The intervention of CB[7] affect effectually photochromic properties of the guest such as $\Phi_{E\rightarrow Z}$ and $\Phi_{Z\rightarrow E}$. Photoisomerization quantum yied from (*E*)-form to (*Z*)-form ($\Phi_{E\rightarrow Z}$) of WS-SSP/CB[7] was determined to be 6.14% ± 0.07%, which was less than that of the only guest (12.38% ± 0.04%), while $\Phi_{Z\rightarrow E}$ of the assembly (7.20% ± 0.10%) was superior to that of WS-SSP (3.46% ± 0.05%). Furthermore, photoisomerization speed of WS-SSP/CB[7] from (*E*)-isomer to (*Z*)-isomer was slower than that of the free guest, because photoisomerized process of (*E*)-WS-SSP in the assembly need to overcome the obstacles of macrocyclic host, resulting in the assembly having a smaller quantum yield (*E*→*Z*) than the guest alone. The assembly pattern of (*Z*)-WS-SSP and CB[7] was characterized by their ^{1}H NMR titration and contrast (Figs. S14 and S15 in Supporting information) and indicated the moieties of quaternary ammonium salt and the benzene ring attached to it were encapsulated in the cavity of CB[7], as was illuminated in Scheme 1. The complex stability constant (K_s) was calculated as 8.5×10^4 L/mol (K_{S1}), 7.5×10^4 L/mol (K_{S2}) at 25 °C using a nonlinear least-squares curve-fitting method by analyzing the continuous changes in the absorbance of (*Z*)-WS-SSP at 225 nm in the presence of varying concentrations of CB[7] (Fig. S18 in Supporting information) [37]. As similar as its (*E*)-isomer, (*Z*)-WS-SSP displayed apparent fluorescence enhancement upon sequential addition of CB[7] (Fig. S19 in Supporting information). Furthermore, great differences in fluorescence intensity exist in the different isomers (Fig. S7b). These significant discoveries inspired us to investigate photo-induced fluorescence switching behaviors of the water-soluble supramolecular complex. Just as we expected, we employed 311 nm and 385 nm light as stimulating factors to conduct light experiments. As discerned in Fig. 4a, photoluminescence intensity of (*E*)-WS-SSP/CB[7] at emission maximum (440 nm) was quenched by 70% upon irradiation at 311 nm light for 120 s. Subsequent 385 nm light irradiation of the irradiated sample for 32 s achieved restoration of 59% initial fluorescence intensity (Fig. 4b). Afterwards, three cycles were carried

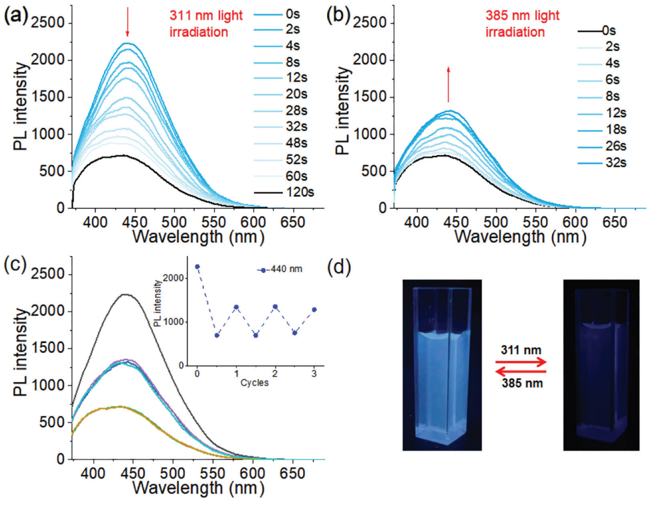

Fig. 4. (a) Photoluminescence spectral variation of (*E*)-WS-SSP/CB[7] upon irradiation at 311 nm light; (b) Photoluminescence spectral variation of **a** upon irradiation at 385 nm light; (c) Photoluminescence spectral variation of (*E*)-WS-SSP/CB[7] upon irradiation at alternating 311 nm and 385 nm light (Inset: The alteration of photoluminescence intensity of (*E*)-WS-SSP/CB[7] at 440 nm upon irradiation at alternating 311 nm and 385 nm light); (d) The alteration of fluorescence photograph of (*E*)-WS-SSP/CB[7] under 365 nm light upon irradiation at alternating 311 nm and 385 nm light; [CB[7]] = 2[(*E*)-WS-SSP] = 4.0×10^{-5} mol/L, $\lambda_{ex} = 350$ nm.

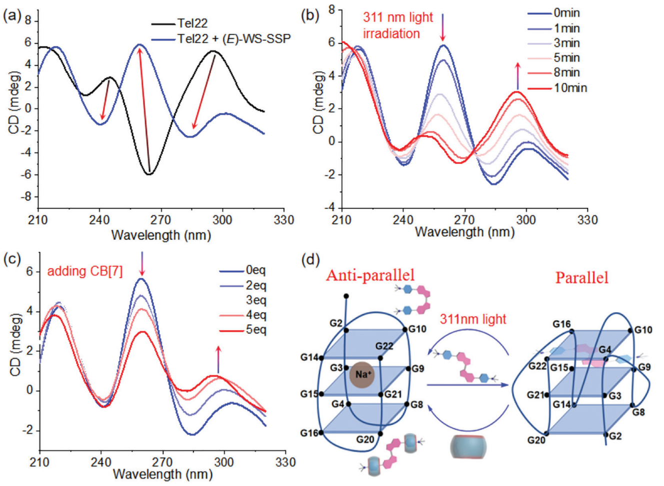

Fig. 5. (a) CD spectra of Tel22 and (*E*)-WS-SSP/Tel22; (b) CD spectral variation of (*E*)-WS-SSP/Tel22 upon irradiation at 311 nm light; (c) CD spectral variation of (*E*)-WS-SSP/Tel22 incubation with CB[7]; (d) The illustration for Schematic diagram of anti-parallel/parallel G-quadruplex structure of Tel22 regulated by (*E*)-WS-SSP. [Tel22] = 2.0×10^{-5} mol/L; [(*E*)-WS-SSP] = 1.25×10^{-4} mol/L, all samples containing 0.1 mol/L Na^+.

out at least and fluorescence photograph was alternately lighted on and off in above process (Figs. 4c and d), manifesting good fluorescence photoswitching repeatability. Besides, the only guest WS-SSP also possessed good fluorescence photoswitching performance (Fig. S16 in Supporting information). In consequence, the supramolecular assembly developed by us might regard as a novel photoresponsive intelligent photoluminescence material.

Because of the extremely important physiological functions and multiple secondary structures of telomere structure, (*E*)-WS-SSP was used to regulate the different structures of telomere. It has been reported that human telomeric repeat Tel22 (5'-AGGGTTAGGGTTAGGGTTAGGG-3') shows anti-parallel structure in aqueous solution [38]. Afterwards, crystal structure of parallel quadruplexes from same telomeric DNA sequence was reported in 2002 [39]. Because diverse G-quadruplex structures may have distinct physiological functions, scientists try to search methods to regulate G-quadruplex structures. In the presence of sodium ions, Tel22 exhibited an anti-parallel G-quadruplex structure. Interestingly, after incubating with (*E*)-WS-SSP, the decrease of the peak at 295 nm and increase of the peak at 265 nm in circular dichroism (CD) spectra indicated that the G-quadruplex structure had been changed from anti-parallel to parallel (Fig. 5a). This result manifested that (*E*)-WS-SSP could regulate G-quadruplex structure under physiological conditions. In order to further verify that the modulating effect was attributed to (*E*)-configuration of WS-SSP but not its (*Z*)-form, 311 nm light was used to irradiate the Tel22/(*E*)-WS-SSP sample. Interestingly, as displayed in Fig. 5b, time-dependence enhancement of the peak at 295 nm and decline of the peak at 265 nm indicated that anti-parallel G-quadruplex structure was regenerated, which was originated from conversion of (*E*)-WS-SSP to its (*Z*)-configuration in above irradiating process. Moreover, CB[7] could expediently assemble with (*E*)-WS-SSP to form a supramolecular complex (*E*)-WS-SSP/CB[7] *via* simply mixing them together. Therefore, CB[7] could be also employed to interfere with regulation effect of (*E*)-WS-SSP on G-quadruplex structure. As expected, when the Tel22/(*E*)-WS-SSP sample was added with CB[7], the initial anti-parallel G-quadruplex structure recovered to some extent (Fig. 5c). Hence, as illustrated in Fig. 5d, (*E*)-WS-SSP could induce transformation of anti-parallel G-quadruplexes toparallel structure even in a physiological environment containing sodium ions. However, when (*E*)-WS-SSP was transformed to its (*Z*)-configuration or the binding site in its (*E*)-configuration was hiddened and invalided *via* host-guest complexation, the anti-parallel G-quadruplex structure would be reformed to some extent. Therefore, the water-soluble photoswitch could modulate selectively and controllably G-quadruplex structure of Tel22 through light irradiation and host-guest complexation.

In summary, we designed and prepared a water-soluble stiff-stilbene molecular photoswitch WS-SSP through several simple steps, which could assemble with CB[7] to construct a 1:2 supramolecular complex WS-SSP/CB[7]. WS-SSP could conduct photoisomerization between its (*E*)- and (*Z*)-configuration, and exhibited good reversibility, when irradiated at alternating 311 nm and 385 nm light. Furthermore, the inclusion of CB[7] on the guest WS-SSP induced its fluorescence enhancement *via* host-guest complexation. Simultaneously, introduction of CB[7] resulted in decline of $\Phi_{E\rightarrow Z}$ and elevation of $\Phi_{Z\rightarrow E}$ of the stiff-stilbene, and the assembly still remained good photochromic feature. In consequence, it is crucial that fluorescence of the supramolecular assembly could be switched on/off upon irradiation with distinct light. In addition, the water-soluble photoswitch developed by us could be used to modulate G-quadruplex structure of Tel22 from anti-parallel to parallel in physiological environment. Besides, the parallel G-quadruplex structure induced by (*E*)-WS-SSP above might be further regulated to its initial state through light stimulation and host-guest complexation. The work provided a new tunable and convenient method for adjusting photochromic characteristics of molecular switches and developing smart materials which were prospectively applied in modulating G-quadruplex structure, bioimaging and anti-counterfeiting.

Declaration of competing interest

The authors declare that they have no known competing financial interests or personal relationships that could have appeared to influence the work reported in this paper.

Acknowledgments

We thank Top-Notch Talents Program of Henan Agricultural University (No. 30501049), Project supported by the Science and Technology Department of Henan Province (No. 212102310332) and the Merit Funding for the Oversea Staff of Henan Province for financial support.

Supplementary materials

Supplementary material associated with this article can be found, in the online version, at doi:10.1016/j.cclet.2022.108108.

References

[1] H.Y. Zhou, Q.S. Zong, Y. Han, C.F. Chen, Chem. Commun. 56 (2020) 9916–9936.
[2] L. Zhang, Y.M. Zhang, G.X. Liu, Y. Liu, Chin. Chem. Lett. 30 (2019) 120–122.
[3] X. Wu, L. Gao, J.Z. Sun, X.Y. Hu, L.Y. Wang, Chin. Chem. Lett. 27 (2016) 1655–1660.
[4] Y.M. Zhang, Y.H. Liu, Y. Liu, Adv. Mater. 32 (2020) 1806158.
[5] Y. Zhou, Y. Chen, P.P. Zhu, et al., Chem. Commun. 53 (2017) 3681–3684.
[6] C. Wang, Y.M. Zhang, H. Li, et al., Chin. Chem. Lett. 33 (2022) 2447–2450.
[7] T. Cui, G. Liu, W. Zhang, et al., Chin. Chem. Lett. 32 (2021) 357–361.
[8] D.A. Xu, Q.Y. Zhou, X. Dai, et al., Chin. Chem. Lett. 33 (2022) 851–854.
[9] H. Nie, Z. Wei, X.L. Ni, Y. Liu, Chem. Rev. 122 (2022) 9032–9077.
[10] T. Xiao, H. Qian, Y. Shen, et al., Mater. Today Chem. 24 (2022) 100833.
[11] T. Xiao, J. Wang, Y. Shen, et al., Chin. Chem. Lett. 32 (2021) 1377–1380.
[12] T. Xiao, W. Zhong, L. Zhou, et al., Chin. Chem. Lett. 30 (2019) 31–36.
[13] G. Liu, J. Zhu, Y. Zhou, et al., Org. Lett. 20 (2018) 5626–5630.
[14] G. Liu, L. Wang, Y. Zhou, et al., Dyes Pigments 172 (2020) 107800.
[15] Z.Q. Cao, D.P. Wu, M.Z. Li, et al., Chin. Chem. Lett. 33 (2022) 1533–1536.
[16] J. Yao, W. Wu, W. Liang, et al., Angew. Chem. Int. Ed. 56 (2017) 6869–6873.
[17] W. Liu, G. Liu, X. Zhu, et al., New J. Chem. 46 (2022) 8062–8068.
[18] J. Volarić, W. Szymanski, N.A. Simeth, B.L. Feringa, Chem. Soc. Rev. 50 (2021) 12377.

[19] Q.L. Yu, Y.M. Zhang, Y.H. Liu, X. Xu, Y. Liu, Sci. Adv. 4 (2018) 2297.
[20] G. Liu, Y.M. Zhang, X. Xu, et al., Adv. Opt. Mater. 5 (2017) 1700770.
[21] H. Chen, X. Ma, S. Wu, H. Tian, Angew. Chem. Int. Ed. 53 (2014) 14149–14152.
[22] C. Jia, A. Migliore, N. Xin, et al., Science 352 (2016) 1443–1445.
[23] Z. Li, Y. Dai, Z. Lu, et al., Chem. Commun. 55 (2019) 13430–13433.
[24] G. Liu, H. Zhang, X. Xu, et al., Mater. Today Chem. 22 (2022) 100628.
[25] G. Liu, X. Xu, Y. Chen, et al., Chem. Commun. 52 (2016) 7966–7969.
[26] Z. Li, S. Chen, Y. Huang, et al., Chem. Eng. J. 450 (2022) 138087.
[27] K. Higashiguchi, G. Taira, J.I. Kitai, T. Hirose, K. Matsuda, J. Am. Chem. Soc. 137 (2015) 2722–2729.
[28] D. Villarln, S.J. Wezenberg, Angew. Chem. Int. Ed. 59 (2020) 13192–13202.
[29] S.J. Wezenberg, M. Vlatković, J.C.M. Kistemaker, B.L. Feringa, J. Am. Chem. Soc. 136 (2014) 16784–16787.
[30] M. Vlatković, B.L. Feringa, S.J. Wezenberg, Angew. Chem. Int. Ed. 55 (2016) 1001–1004.
[31] S.J. Wezenberg, B.L. Feringa, Org. Lett. 19 (2017) 324–327.
[32] J. Leng, G. Liu, T. Cui, et al., Dyes Pigments 184 (2021) 108838.
[33] S.J. Barrow, S. Kasera, M.J. Rowland, J.d. Barrio, O.A. Scherman, Chem. Rev. 115 (2015) 12320.
[34] G. Liu, X. Xu, X. Dai, et al., Mater. Horiz. 8 (2021) 2494–2502.
[35] G. Liu, Y.M. Zhang, C. Wang, Y. Liu, Chem. Eur. J. 23 (2017) 14425–14429.
[36] G. Liu, J. Leng, Q. Zhou, et al., Dyes Pigments 203 (2022) 110361.
[37] P. Thordarson, Chem. Soc. Rev. 40 (2011) 1305–1323.
[38] Y. Wang, D.J. Patel, Structure 1 (1993) 263–282.
[39] G.N. Parkinson, M.P.H. Lee, S. Neidle, Nature 417 (2002) 876–880.